American Mineralogist, Volume 95, pages 1000–1005, 2010

In situ ultrasonic velocity measurements across the olivine-spinel transformation in Fe_2SiO_4

Qiong Liu,* Wei Liu, Matthew L. Whitaker, Liping Wang, and Baosheng Li

Mineral Physics Institute, Stony Brook University, Earth & Space Sciences Building, Stony Brook, New York 11794-2100, U.S.A.

Abstract

Compressional (P) and shear (S) wave velocities across the olivine-spinel transformation in Fe_2SiO_4 were investigated in situ using combined synchrotron X-ray diffraction, X-ray imaging, and ultrasonic interferometry up to 5.5 GPa along the 1173 K isotherm. The onset of the spinel to olivine transformation at 4.5 GPa and olivine to spinel transition for Fe_2SiO_4 at 4.8 GPa was concurrently observed from X-ray diffraction, the amplitude of the ultrasonic signals, the calculated velocities, and the ratio of P and S wave velocities (v_P/v_S). No velocity softening was observed prior to the fayalite to spinel transition. The velocity contrasts across the Fe_2SiO_4 spinel to fayalite phase transition are derived directly from the measured velocities, which are 13 and 12% for P and S waves, respectively, together with a density contrast of 9.4%. A comparison with literature data indicates that the changes in compressional-wave velocity and density across the olivine-spinel transformation in Fe_2SiO_4 are comparable to those with different iron concentrations in the $(Mg,Fe)_2SiO_4$ solid solution, whereas the shear wave velocity contrast decreases slightly with increasing iron concentration.

Keywords: Olivine-spinel, phase transformation, Fe_2SiO_4, velocity contrasts, ultrasonic measurements, iron concentration

Introduction

Olivine, $(Mg,Fe)_2SiO_4$, is the most abundant mineral in the upper mantle. Its polymorphic transformations from olivine to wadsleyite and wadsleyite to ringwoodite are believed to be responsible for the seismically observed discontinuities at 410 and 520 km depths. The transformation pressure, kinetics, density, and elasticity variations associated with these transitions are critical to understanding the depth, sharpness, and amplitude of these discontinuities and hence the composition, structure, and dynamics of the Earth's mantle (Bass and Anderson 1984; Weidner 1985; Bina and Wood 1987; Ita and Stixrude 1992; Stixrude 1997; Li et al. 1998; Weidner and Wang 2000; Cammarano et al. 2005a, 2005b). In addition, as suggested by experimental studies (Sung and Burns 1976a, 1976b; Burnley and Green 1989; Burnley et al. 1991, 1995; Wu et al. 1993; Rubie and Ross 1994) and seismic data (Iidaka and Suetsugu 1992; Pankow et al. 2002; Jiang et al. 2008), olivine may persist metastably to depths well below the equilibrium phase boundary subduction zones due to the lower temperature. Therefore, the physical properties associated with the polymorphic phase transitions of olivine also play an important role in modeling the behavior of subducting slabs.

Fayalite, the iron end-member of the $(Mg,Fe)_2SiO_4$ solid-solution series, transforms directly into the spinel phase at ~5 GPa, 1073–1173 K (Akimoto et al. 1967; Yagi et al. 1987) without transforming into a wadsleyite phase at intermediate pressures as for Mg-rich compositions in this series. While there is abundant literature on the elastic properties of the Mg-rich olivine and its polymorphs, the elasticity of the fayalite and spinel phase of Fe_2SiO_4, is still not well constrained. Although olivine at Earth's upper mantle conditions typically has Fe/(Fe+Mg) ~ 0.1–0.13, measurements on the iron end-member will facilitate the understanding of the effect of iron on the density and elastic properties of olivine and its high-pressure phases, the mechanism and characteristics of the polymorphic phase transformations, and the calculation of mantle phase equilibria (e.g., Stixrude and Lithgow-Bertelloni 2005). Moreover, studies on the Fe_2SiO_4 end-member provide useful information on oxygen fugacity of the upper mantle.

Many previous studies have evaluated the velocity jumps across the polymorphic phase transitions of olivine based on extrapolations using pressure and temperature derivatives obtained for individual phases from experiments at high pressure and room temperature, or high temperature and ambient pressure. Direct velocity measurements on these phases under simultaneous high-pressure and high-temperature conditions comparable to those in the mantle are still scarce [Liu et al. (2008) and references therein], especially for olivine with magnesium-rich compositions, which require higher pressure and temperature conditions for the phase transitions than iron-rich compositions. There is great advantage for conducting in situ measurements across the transition from the low-pressure phase to high-pressure phase; it not only provides data for the change in physical properties across the phase transition, but also allows for a direct investigation of the dynamic features associated with the transition, such as elastic anomalies (softening, attenuation, if any) prior to, during, and after the transition as observed in pyroxene (Jackson et al. 2004; Kung et al. 2004, 2006), stishovite (Shieh et al. 2002), α and β

* Present address: Key Laboratory of Orogenic Belt and Crustal Evolution, School of Earth and Space Sciences, Peking University, Beijing, 100871, China. E-mail: qiong.liu@pku.edu.cn

0003-004X/10/0007–1000$05.00/DOI: 10.2138/am.2010.3369

quartz (Lakshtanov et al. 2007), and even fayalite (Speziale et al. 2004). Li and Weidner (2008) showed softening of P-wave velocities within the two phase region of olivine-ringwoodite in olivine with Fa_{70} composition. Moreover, the existing studies on phase transitions and elasticities were conducted either at room temperature (Kung et al. 2004, 2006) or room pressure (Lakshtanov et al. 2007; Jackson et al. 2004; Speziale et al. 2004), which is significantly different from the conditions found in the mantle. Therefore, in situ elasticity measurements at elevated temperature and pressure are required.

For iron end-member olivine, the occurrence of a phase transition at relatively low pressures compared to Mg-rich compositions makes it a good candidate for in situ measurements of acoustic velocities across the phase transition. Fukizawa and Kinoshita (1982) conducted in situ measurements on shear wave velocities of polycrystalline Fe_2SiO_4 olivine and spinel up to 5.2 GPa and to 973 K and observed an 11% velocity jump at 5.2 GPa and 923 K. Unfortunately, due to the lack of in situ monitoring of the progress of the phase transition, nearly 40% of the sample remained as olivine as discovered after the experiment (Fukizawa and Kinoshita 1982). In this study, by using a high-pressure apparatus equipped with simultaneous ultrasonic interferometry, synchrotron X-ray diffraction, and X-ray imaging techniques (Li et al. 2004), we can conduct simultaneous measurements of P and S wave velocities and density across this phase transformation at high pressure and high temperature, as well as monitor the progress and completion of the phase transformation. We report the P and S wave velocities and velocity contrasts, density contrasts, and impedance contrasts for the Fe_2SiO_4 spinel to fayalite phase transition and the reverse transition up to 5.5 GPa along the 1173 K isotherm.

Experimental methods

The fayalite starting material was synthesized by Donald Lindsley [see Liu et al. (2008) for details]. To fabricate a specimen suitable for acoustic velocity measurements, the fayalite powder was packed in an iron capsule and hot-pressed in a 1000 ton uniaxial split-cylinder apparatus (USCA-1000) at ~4 GPa, 1073 K for 1 h. The recovered polycrystalline sample (length = 0.79 mm, OD = 1.9 mm, 98.9% theoretical density) was confirmed to be a single phase of fayalite by synchrotron X-ray diffraction at beamline X17B2 of National Synchrotron Light Source (NSLS) in Brookhaven National Laboratory (BNL).

Velocity measurements at high pressure and high temperature were conducted in a cubic anvil press (SAM85) installed at X17B2 at BNL. The experimental setup and the technique for ultrasonic interferometry are described in detail elsewhere (Li et al. 2004). Briefly, the sample was placed in the center of a boron epoxy cube (6.4 mm edge length), which was used as a pressure-transmitting medium, with NaCl and BN mixture (10:1 by weight) as surrounding material to provide a pseudo-hydrostatic pressure environment. A dense alumina rod (2.5 mm in diameter, 2.0 mm in length) with flat surfaces polished to be parallel within 0.05° was inserted into the boron epoxy cube and used as an acoustic buffer rod to optimize the acoustic energy propagating from the anvil into the sample. The sample temperature was monitored by a W3%Re-W25%Re thermocouple placed next to the sample.

The experimental *P-T* path is shown in Figure 1. The sample was first pressurized at room temperature to ~2.8 GPa and then heated to ~573 K to anneal the sample and minimize the deviatoric stress (labeled as paths 1, 2, and 3 in Fig. 1). This procedure also minimizes the possibility of deforming the sample in subsequent cold compression (path 4). At the peak pressure of 8.7 GPa, as well as during decompression, multiple heating/cooling cycles to 673 K were performed to provide a dense coverage in pressure and temperature space. This portion of the data (paths 1–15, and part of path 17, Fig.1) was collected primarily for a *P-V-T*-EOS study on the fayalite phase, and the results will be presented elsewhere (Liu et al. manuscript in preparation). After the pressure was decreased to 2.7 GPa, the sample was heated to 973 K, followed by an isothermal compression to a peak pressure of 5 GPa (path 17). While maintaining a constant hydraulic load at the peak pressure, the temperature was increased from 973 to 1073 K, and subsequently to 1173 K, (paths 18, 19) (Fig. 2). After that, isothermal decompression along 1173 K (path 20) was performed to transform the sample to fayalite followed by an attempt to reverse the transition by an isothermal compression up to 5.1 GPa (path 21).

Energy-dispersive X-ray diffraction data were collected using a solid-state Ge detector for phase identification and pressure calculation. The incident X-ray beam was collimated to 0.1 × 0.1 mm and the diffraction angle was set at $2\theta = 6.56°$. The phase transformation process between fayalite and spinel was monitored by the appearance/disappearance of spinel/fayalite peaks in the X-ray diffraction patterns. Specifically, for the transition from fayalite to spinel, the formation of Fe_2SiO_4 spinel was identified by the appearance of three characteristic diffraction lines at (220), (400), and (331), which are free of obstruction by fayalite peaks or Pb fluorescence peaks; whereas for the transition from spinel to fayalite, the appearance of fayalite phase was identified by four diffraction lines (111), (031), (222), and (042) whose positions were not overlapped with the spinel phase (Fig. 2). The pressure on the sample was determined by using NaCl as an internal pressure standard and a Decker equation of state (Decker 1971).

Two-way travel times of ultrasonic waves through the sample were acquired using the transfer function method (Li et al. 2002) with a dual mode lithium niobate ($LiNbO_3$) transducer (10° Y-cut, 30 MHz for S wave and 50 MHz for P wave). A broadband pulse (20–70 MHz) was transmitted and received by the piezoelectric transducer; the round-trip propagation time inside the sample was obtained by measuring the time delay between two consecutive echoes reflected from the front and rear surfaces of the sample. P and S wave travel times were determined simultaneously with one standard deviation of ~0.2 and ~0.4 ns, respectively. Sample length was monitored by the X-ray radiographic imaging system that consisted of a YAG crystal, a mirror and a CCD camera (Li et al. 2004). As demonstrated in previous study, without interpolation, the sample length can be measured within one pixel (Li et al. 2004), which gives a precision better than 0.4% for the sample used in this study (~395 pixels).

Results and discussion

The X-ray diffraction patterns at pressures near the phase transition along isothermal compression/decompression were carefully examined to identify the phases present in the sample. Upon increasing pressure at a constant temperature of 973 K (path 17 in Fig. 1), the sample remained as fayalite phase until a trace amount of spinel was detected at ~4.1 GPa. However, up to the peak pressure of 5.0 GPa, complete transformation from fayalite to spinel at this temperature was unsuccessful due to the sluggish kinetics. To ensure the sample transformed to pure spinel

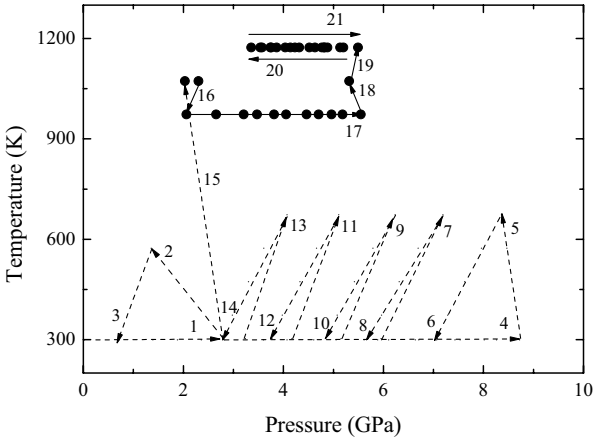

Figure 1. Experimental *P-T* path indicating the loading and subsequent heating/cooling cycles (dashed lines with arrows) before the isothermal (973, 1073, and 1173 K) phase transformation processes reported in this study (solid circles).

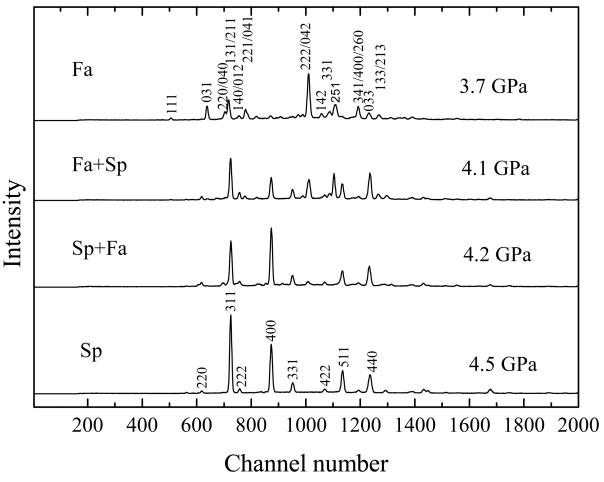

FIGURE 2. Examples of X-ray diffraction patterns for the Fe_2SiO_4 sample show a transition sequence from a single-phase spinel (bottom) to a single phase of olivine (top) during the 1173 K isothermal decompression. The x-axis is the channel number. The y-axis is the arbitrary intensity units.

phase, the temperature was then increased to a final temperature of 1173 K (path 19) (Fig. 1), and the complete transformation to spinel was confirmed by X-ray diffraction.

When decompressed along the 1173 K isotherm, the sample remained in the spinel phase from 5.5 to 4.5 GPa. Fayalite peaks started to appear at 4.2 GPa and fayalite became the only phase after further decompression to 3.7 GPa. By comparison, during the subsequent re-pressurization along the same isotherm (path 21, Fig. 2) to transform the sample back to spinel, fayalite remained as the only phase up to ~4.8 GPa and completely transformed to spinel at ~4.9 GPa. The observed behavior whereby higher pressures (4.8–4.9 GPa) are required to transform olivine to spinel than those (4.2–3.7 GPa) for the reverse transformation could be described as hysteresis. A comparison of the observations along the 973 and 1173 K isotherms indicated that the transition pressure from fayalite to spinel at 1173 K is ~0.8–0.9 GPa higher than that at 973 K. This yields a Clapeyron slope of dP/dT = 0.004 to 0.0045 GPa/K, which is consistent with previous observations for this phase transition (Akimoto et al. 1967). It is also noted that along 1173 K, the onset of the transition from spinel to fayalite (~4.2 GPa) is 14% (0.6 GPa) lower than that of the transition from fayalite to spinel (~4.9 GPa). A similar phenomenon was observed by Yagi et al. (1987) who reported that the transition from fayalite to spinel did not occur until the pressure was ~20% greater than the equilibrium transition pressure at 1073 and 1173 K.

The compressional and shear wave velocities along three isotherms are summarized in Table 1 and Figures 3 and 4. At 973 K, both P and S wave velocities increase smoothly with increasing pressure up to 5.2 GPa followed by a faster velocity increase to 5.6 GPa (Fig. 3). Although the spinel peaks started to appear in the X-ray diffraction pattern at 5.0 GPa and 973 K, due to the kinetics effect, the proportion of the spinel phase was not significant enough to cause a large velocity increase. From these data, a pressure derivative of ~0.022 km/s GPa^{-1} was obtained for the shear-wave velocity, which is comparable to those observed for other mantle minerals, such as wadsleyite [0.020 km/s GPa^{-1}, Liu et al. (2009)]. This suggests that the shear velocity of fayalite did not exhibit obvious softening before its phase transition to the spinel phase. This conclusion was supported by the shear-wave velocity study on polycrystalline Fe_2SiO_4 at simultaneous high pressure and high temperature up to 5.2 GPa and 973 K by Fukizawa and Kinoshita (1982) where no anomalous decrease in shear-wave velocity was observed at the olivine to spinel transformation. In addition, Webb et al. (1984) found that there is no evidence of premonitory pressure-induced softening of the elastic stiffness modulus c_{55} in single-crystal fayalite. The softening observed in previous studies at room temperature in shear modulus (Speziale et al. 2004) may be related to pressure induced amorphization (Richard and Richet 1990) rather than phase transition to spinel.

Even though there are only three data points along the 1073 K isotherm, a clear jump in velocity is shown between 2.3–5.3 GPa (Figs. 3 and 4). Along the 1173 K isotherm, when the pressure was decreased from 5.5 GPa, both P and S wave velocities decrease with decreasing pressure to ~4.5 GPa, at which point a rapid drop was observed (points 4–6, Figs. 3 and 4), followed by a moderate decrease with further decrease of pressure to 3.4 GPa. The sudden velocity decrease at ~4.5 GPa marks the phase transition from spinel to fayalite, which is supported by synchronous observation of changes in the amplitudes of the ultrasonic signals, as well as the appearance of the fayalite peaks in the X-ray diffraction pattern.

TABLE 1. Experimental data on Fe_2SiO_4 phase transformation at 973, 1073, and 1173 K

	T (K)	P (GPa)	$2t_P$ (ms)	$2t_S$ (ms)	l (mm)	v_P (km/s)	v_S (km/s)
	973	2.064	0.2404	0.4816	0.8139	6.771	3.380
	973	2.657	0.2386	0.4786	0.8114	6.802	3.391
	973	3.209	0.2370	0.4760	0.8104	6.839	3.405
	973	3.473	0.2360	0.4746	0.8074	6.843	3.403
	973	3.814	0.2346	0.4728	0.8084	6.892	3.420
	973	4.055	0.2338	0.4716	0.8064	6.899	3.420
	973	4.465	0.2326	0.4700	0.8069	6.938	3.434
	973	4.703	0.2318	0.4688	0.8064	6.958	3.440
	973	4.962	0.2306	0.4672	0.8035	6.968	3.439
	973	5.184	0.2276	0.4610	0.7975	7.008	3.460
	973	5.551	0.2244	0.4556	0.7985	7.116	3.505
	1073	2.032	0.2444	0.4898	0.8164	6.681	3.334
	1073	2.302	0.2426	0.4868	0.8124	6.698	3.338
	1073	5.315	0.1980	0.4052	0.7745	7.824	3.823
Sp→Fa	1173	5.495	0.1972	0.4050	0.7696	7.805	3.800
	1173	5.201	0.1972	0.4046	0.7656	7.764	3.784
	1173	4.821	0.1976	0.4048	0.7611	7.703	3.760
	1173	4.522	0.1982	0.4052	0.7621	7.690	3.762
	1173	4.232	0.2028	0.4140	0.7686	7.580	3.713
	1173	4.141	0.2296	0.4664	0.7780	6.777	3.336
	1173	3.739	0.2328	0.4712	0.7825	6.723	3.321
	1173	3.54	0.2358	0.4812	0.7845	6.654	3.261
	1173	3.357	0.2368	0.4842	0.7835	6.618	3.236
Fa→Sp	1173	3.575	0.2348	0.4770	0.7830	6.670	3.283
	1173	3.866	0.2332	0.4746	0.7815	6.703	3.293
	1173	3.757	0.2330	0.4740	0.7805	6.700	3.293
	1173	4.04	0.2318	0.4726	0.7805	6.734	3.303
	1173	4.318	0.2308	0.4714	0.7800	6.759	3.309
	1173	4.632	0.2296	0.4694	0.7785	6.782	3.317
	1173	4.817	0.2282	0.4696	0.7775	6.814	3.311
	1173	4.771	0.2058		0.7631	7.416	
	1173	4.883	0.1968		0.7591	7.714	
	1173	5.136	0.1922		0.7551	7.858	

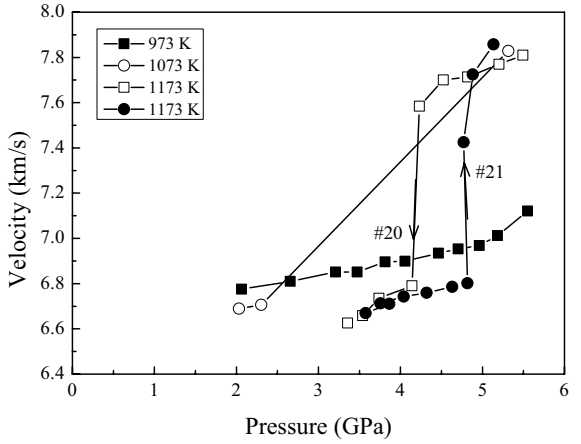

FIGURE 3. P wave velocities for Fe_2SiO_4 phases as a function of pressure at 973, 1073, and 1173 K. The lines connecting the symbols are used for guiding the eyes. The uncertainties in the measured velocities are ~0.5%.

In the course of reversing the above transformation along *P-T* path 21 in Figure 1, both P and S wave velocities were found to increase with increasing pressure up to ~4.8 GPa (Figs. 3 and 4, points a–g) while the sample remained as fayalite phase. Above 4.8 GPa, the phase transition from fayalite to spinel was evident in the recorded X-ray diffraction pattern, accompanied by a change in the ratio of the amplitudes of the acoustic signals from the buffer rod and the sample (A_{Sample}/A_{BR}), as well as a rapid increase in the P wave velocity (Fig. 3, points g–i). The S wave signal from the sample, however, experienced significant reduction in the signal-to-noise ratio during the phase transition. This might be caused by the degradation of the flatness and/or the parallelism of the sample surfaces after going through multiple phase transitions. As a result, no reliable S wave velocities on the final spinel phase were available for comparison in Figure 4.

Unit-cell refinement of the X-ray diffraction data between 4.5 and 3.7 GPa indicated a density contrast of 9.4% across the phase transition. This result is in good agreement with the density contrast (9.1%) at 5.3 GPa, 1273 K reported by Yagi et al. (1987) using in situ observation using synchrotron X-ray diffraction. Since the transition from hexagonal close-packed (hcp) (fayalite) to cubic close-packed (ccp) (spinel) anion arrays does not change the coordination number of the cations with oxygen ions, the large density contrast for the fayalite-spinel transformation has been attributed to the difference in the atomic structures of the two phases (Kamb 1968). Namely, the stabilization of spinel as well as the increase of density is attributed to the expansion of the edges shared between coordination octahedra relative to the unshared edges to meet the required cation-anion interatomic distances.

The velocity contrast across the transformation was calculated using $2[v_1 - v_2)/(v_1 + v_2)]$, where v_1 and v_2 were the ultrasonic velocities at two nearest experimental pressures with only pure fayalite (P_1) and pure spinel (P_2) in the recorded X-ray diffraction pattern. From the spinel to fayalite transition at 1173 K, the measured velocities at 4.5 GPa for spinel and 3.7 GPa for fayalite yielded velocity contrasts of ~13 and ~12% for P and S waves, respectively. The resulting P and S wave impedance contrasts are 23 and 22%, respectively. For the subsequent transition from fayalite to spinel, the directly measured velocity contrast for P waves at 4.8–4.9 GPa, 1173 K is 13%, which coincides with that of the reverse transformation. The velocity contrast obtained in the current study is in good agreement with the result by Fukizawa and Kinoshita (1982). They observed an 11% shear-wave velocity jump at 5.2 GPa and 923–948 K where the olivine was partially (~60%) transformed to spinel, from which a velocity jump of 14% (13.1% velocity contrast) was inferred if the Fe_2SiO_4 olivine was completely transformed to spinel at this pressure and temperature.

To gain insights on the effect of iron on the change in physical properties across the fayalite-spinel transition, the density and velocity contrasts of $(Mg,Fe)_2SiO_4$ olivine as a function of iron content are compared in Table 2. At ambient conditions, the density contrast is completely independent of iron content. The current result of density contrast is slightly lower than those at ambient conditions, presumably due to the increased incompressibility of the spinel structure, which consists of a three-dimensional edge-sharing framework of octahedra in contrast to the one-dimensional columns of octahedra in olivine. Within the range of the previous values, the velocity contrast for P waves can be considered nearly independent of iron concentration. Based on the current results from the spinel to fayalite transition at 4.5–3.7 GPa and the fayalite to spinel transition at 4.8–4.9 GPa, it appears to suggest that the P-wave velocity contrast is also independent of pressure, although the current result at elevated pressure is close to the lower bound of the reported value at ambient pressure. The S-wave velocity contrast obtained in this study, on the other hand, is in complete agreement with that reported by Rigden and Jackson (1991) for the fayalite-spinel transition, indicating there is no dependence on pressure and temperature. However, when compared with magnesium-rich compositions, the velocity contrast of S wave decreases with iron concentration, which can be modeled as $\Delta v_S = 17–5.0x$ with x being the molar fraction of iron. This implies that variations in iron content in the transition zone will produce large variations in shear-wave velocity jump but with nearly constant

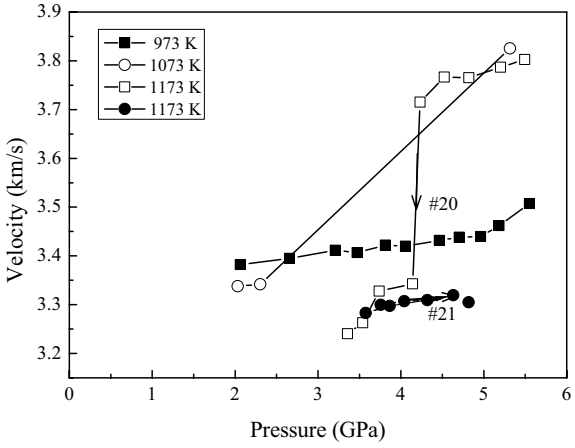

FIGURE 4. S wave velocities for Fe_2SiO_4 phases as a function of pressure at 973, 1073, and 1173 K. The uncertainties in the measured velocities are ~0.5%.

TABLE 2. Elastic property change (in %) across olivine-spinel transition as a function of iron content*

X_{Fe}	$\Delta\rho$	Δv_P	Δv_S	ref†
0	10	16	19	Higo et al. (2006)
0	10	14	15	Li (2003)
0	10	14	16	Rigden et al. (1991)
0.2	10	16	16	Higo et al. (2006)
0.5	10	16	15	Higo et al. (2006)
1	10	19		Mizutani et al. (1970)
1	10	14	11	Rigden and Jackson (1991)
1	10	16	12	Liebermann (1975)
1	9.4	13	12	This study

* All the data are at ambient conditions except those from this study.
† The olivine data for all the compositions are from Chung (1971).

compressional-wave velocity jump, resulting anomalously high $d\ln v_S/d\ln v_P$ across the phase transition.

CONCLUDING REMARKS

We have conducted in situ measurements of the P and S wave velocities and unit-cell volume (density) for the fayalite-spinel phase transition along the 973 and 1173 K isotherms using ultrasonic interferometry in conjunction with synchrotron X-ray diffraction and X-ray imaging. We did not observe softening in shear velocity of fayalite before its phase transition to spinel at high temperatures, and we therefore concluded that the softening observed in previous studies at room temperature in shear modulus may be related to pressure induced amorphization rather than phase transition to spinel. The phase transition at 1173 K is accompanied by a density contrast of ~9.4%. The P wave velocity contrast is ~13% for both the spinel to fayalite transition at 4.5–3.7 GPa and the fayalite to spinel transition at 4.8–4.9 GPa. A comparison of the current results with previous data for $(Mg,Fe)_2SiO_4$ olivine suggests that P wave velocity contrast is approximately independent of pressure and iron concentration. While the S wave velocity contrast from the current study (~12%) for the spinel to fayalite transition is found to be in complete agreement with previous data for Fe_2SiO_4, a comparison with magnesium-rich olivines suggests a decreased S wave velocity contrast with increasing iron content. The density contrasts obtained in this study are comparable to those with different iron concentration in the Mg_2SiO_4-Fe_2SiO_4 solid-solution series at ambient conditions. These findings can be used to gain insights on the compositional variations when compared with seismic tomographic data obtained from 410 to 520 km depths.

ACKNOWLEDGMENTS

The authors thank Donald Lindsley for providing the fayalite powder. This project was supported by NSF grant to B. Li (EAR0635860). We are grateful to Robert Liebermann, Donald Weidner, and Li Li for stimulating discussions. This manuscript was greatly improved by the comments of Ian Jackson and an anonymous referee. The experiment was conducted at X17B2 of NSLS, Brookhaven National Laboratory, which is supported by the U.S. Department of Energy, Office of Science, Office of Basic Energy Sciences, under contract no. DE-AC02-98-CH10886 and by COMPRES, the Consortium for Materials Properties Research in Earth Sciences, under NSF Cooperative Agreement EAR 06-49658, Mineral Physics Institute publication no. 475.

REFERENCES CITED

Akimoto, S.I., Komada, E., and Kushiro, I. (1967) Effect of pressure on melting of olivine and spinel polymorph of Fe_2SiO_4. Journal of Geophysical Research, 72, 679–686.

Bass, J.D. and Anderson, D.L. (1984) Composition of the upper mantle—Geophysical tests of 2 petrological models. Geophysical Research Letters, 11, 237–240.

Bina, C.R. and Wood, B.J. (1987) Olivine-spinel transitions—Experimental and thermodynamic constraints and implications for the nature of the 400 km seismic discontinuity. Journal of Geophysical Research-Solid Earth and Planets, 92, 4853–4866.

Burnley, P.C. (1995) The fate of olivine in subducting slabs: A reconnaissance study. American Mineralogist, 80, 1293–1301.

Burnley, P.C. and Green, H.W. (1989) Stress dependence of the mechanism of the olivine spinel transformation. Nature, 338, 753–756.

Burnley, P.C., Green, H.W., and Prior, D.J. (1991) Faulting associated with the olivine to spinel transformation in Mg_2GeO_4 and its implications for deep-focus earthquakes. Journal of Geophysical Research-Solid Earth and Planets, 96, 425–443.

Cammarano, F., Deuss, A., Goes, S., and Giardini, D. (2005a) One-dimensional physical reference models for the upper mantle and transition zone: Combining seismic and mineral physics constraints. Journal of Geophysical Research-Solid Earth, 110, B01306.

Cammarano, F., Goes, S., Deuss, A., and Giardini, D. (2005b) Is a pyrolitic adiabatic mantle compatible with seismic data? Earth and Planetary Science Letters, 232, 227–243.

Chung, D.H. (1971) Elasticity and equations of state of olivines in Mg_2SiO_4-Fe_2SiO_4 system. Geophysical Journal of the Royal Astronomical Society, 25, 511–538.

Decker, D.L. (1971) High-pressure equation of state for NaCl, KCl, and CsCl. Journal of Applied Physics, 42, 3239–3244.

Fukizawa, A. and Kinoshita, H. (1982) Shear-wave velocity jump at the olivine-spinel transformation in Fe_2SiO_4 by ultrasonic measurements in situ. Journal of Physics of the Earth, 30, 245–253.

Higo, Y., Inoue, T., Li, B.S., Irifune, T., and Liebermann, R.C. (2006) The effect of iron on the elastic properties of ringwoodite at high pressure. Physics of the Earth and Planetary Interiors, 159, 276–285.

Iidaka, T. and Suetsugu, D. (1992) Seismological evidence for metastable olivine inside a subducting slab. Nature, 356, 593–595.

Ita, J. and Stixrude, L. (1992) Petrology, elasticity, and composition of the mantle transition zone. Journal of Geophysical Research: Solid Earth, 97, 6849–6866.

Jackson, J.M., Sinogeikin, S.V., Carpenter, M.A., and Bass, J.D. (2004) Novel phase transition in orthoenstatite. American Mineralogist, 89, 239–244.

Jiang, G.M., Zhao, D.P., and Zhang, G.B. (2008) Seismic evidence for a metastable olivine wedge in the subducting Pacific slab under Japan Sea. Earth and Planetary Science Letters, 270, 300–307.

Kamb, B. (1968) Structural basis of olivine-spinel stability relation. American Mineralogist, 53, 1439–1455.

Kung, J., Li, B.S., and Liebermann, R.C. (2006) Ultrasonic observations of elasticity changes across phase transformations in $MgSiO_3$ pyroxenes. Journal of Physics and Chemistry of Solids, 67, 2051–2055.

Lakshtanov, D.L., Sinogeikin, S.V., and Bass, J.D. (2007) High-temperature phase transitions and elasticity of silica polymorphs. Physics and Chemistry of Minerals, 34, 11–22.

Li, B.S. (2003) Compressional and shear wave velocities of ringwoodite γ-Mg_2SiO_4 to 12 GPa. American Mineralogist, 88, 1312–1317.

Li, B.S., Liebermann, R.C., and Weidner, D.J. (1998) Elastic moduli of wadsleyite (β-Mg_2SiO_4) to 7 Gigapascals and 873 Kelvin. Science, 281, 675–677.

Li, B.S., Chen, K., Kung, J., Liebermann, R.C., and Weidner, D.J. (2002) Sound velocity measurement using transfer function method. Journal of Physics: Condensed Matter, 14, 11337–11342.

Li, B.S., Kung, J., and Liebermann, R.C. (2004) Modern techniques in measuring elasticity of Earth materials at high pressure and high temperature using ultrasonic interferometry in conjunction with synchrotron X-radiation in multi-anvil apparatus. Physics of the Earth and Planetary Interiors, 143–144, 559–574.

Li, L. and Weidner, D.J. (2008) Effect of phase transitions on compressional-wave velocities in the Earth's mantle. Nature, 454, 984–986.

Liebermann, R.C. (1975) Elasticity of olivine (alpha), beta (beta), and spinel (gamma) polymorphs of germanates and silicates. Geophysical Journal of the Royal Astronomical Society, 42, 899–929.

Liu, Q., Liu, W., Whitaker, M.L., Wang, L.P., and Li, B.S. (2008) Compressional and shear wave velocities of Fe_2SiO_4 spinel at high pressure and high temperature. High Pressure Research, 28, 405–413.

Liu, W., Kung, J., Li, B.S., Nishiyama, N., and Wang, Y.B. (2009) Elasticity of $(Mg_{0.87}Fe_{0.13})_2SiO_4$ wadsleyite to 12 GPa and 1073 K. Physics of the Earth and Planetary Interiors, 174, 98–104.

Mizutani, H., Hamano, Y., Ida, Y., and Akimoto, S. (1970) Compressional-wave velocities of fayalite, Fe_2SiO_4 spinel, and coesite. Journal of Geophysical Research, 75, 2741–2747.

Pankow, K.L., Williams, Q., and Lay, T. (2002) Using shear wave amplitude patterns to detect metastable olivine in subducted slabs. Journal of Geophysical Research-Solid Earth, 107(B6), 2108, doi:10.1029/2001JB000608.

Richard, G. and Richet, P. (1990) Room-temperature amorphization of fayalite and high-pressure properties of Fe_2SiO_4 liquid. Geophysical Research Letters, 17, 2093–2096.

Rigden, S.M. and Jackson, I. (1991) Elasticity of germanate and silicate spinels at high-pressure. Journal of Geophysical Research: Solid Earth and Planets, 96, 9999–10006.

Rigden, S.M., Gwanmesia, G.D., Fitz Gerald, J.D., Jackson, I., and Liebermann, R.C. (1991) Spinel elasticity and seismic structure of the transition zone of the mantle. Nature, 354, 143–145.

Rubie, D.C. and Ross, C.R. (1994) Kinetics of the olivine-spinel transformation in subducting lithosphere—Experimental constraints and implications for deep slab processes. Physics of the Earth and Planetary Interiors, 86, 223–241.

Shieh, S.R., Duffy, T.S., and Li, B.S. (2002) Strength and elasticity of SiO_2 across the stishovite–$CaCl_2$-type structural phase boundary. Physical Review Letters, 89, 255507.

Speziale, S., Duffy, T.S., and Angel, R.J. (2004) Single-crystal elasticity of fayalite to 12 GPa. Journal of Geophysical Research-Solid Earth, 109, B12202.

Stixrude, L. (1997) Structure and sharpness of phase transitions and mantle discontinuities. Journal of Geophysical Research: Solid Earth, 102, 14835–14852.

Stixrude, L. and Lithgow-Bertelloni, C. (2005) Thermodynamics of mantle minerals—I. Physical properties. Geophysical Journal International, 162, 610–632.

Sung, C.M. and Burns, R.G. (1976a) Kinetics of high-pressure phase-transformations—Implications to evolution of olivine-spinel transition in downgoing lithosphere and its consequences on dynamics of mantle. Tectonophysics, 31, 1–32.

——— (1976b) Kinetics of olivine→spinel transition: Implications to deep-focus earthquake genesis. Earth and Planetary Science Letters, 32, 165–170.

Webb, S.L., Jackson, I., and Takei, H. (1984) On the absence of shear mode softening in single-crystal fayalite Fe_2SiO_4 at high pressure and room temperature. Physics and Chemistry of Minerals, 11, 167–171.

Weidner, D.J. (1985) A mineral physics test of a pyrolite mantle. Geophysical Research Letters, 12, 417–420.

Weidner, D.J. and Wang, Y. (2000) Phase transformations: Implications for mantle structure. In S. Karato, A.M. Forte, R.C. Liebermann, G. Masters, and L. Stixrude, Eds., Earth's Deep Interior: Mineral physics and tomography from the atomic to the global scale, 117, p. 215–235. Geophysical Monograph, American Geophysical Union, Washington, D.C.

Wu, T.C., Bassett, W.A., Burnley, P.C., and Weathers, M.S. (1993) Shear-promoted phase-transitions in Fe_2SiO_4 and Mg_2SiO_4 and the mechanism of deep earthquakes. Journal of Geophysical Research: Solid Earth, 98, 19767–19776.

Yagi, T., Akaogi, M., Shimomura, O., Suzuki, T., and Akimoto, S. (1987) In situ observation of the olivine-spinel phase-transformation in Fe_2SiO_4 using synchrotron radiation. Journal of Geophysical Research: Solid Earth and Planets, 92, 6207–6213.

Manuscript received August 11, 2009
Manuscript accepted February 9, 2010
Manuscript handled by Artem Oganov